Chapter 6

Comparisons to Tests on Reinforced Concrete Members

Finite element (FE) model predictions of laboratory test results of reinforced concrete members with various confinement methods are presented in this chapter. Five different papers were obtained (none of which were used for the correlations in Chapter 4) that reported tests of confined concrete members. These papers tested a variety of confinement configurations, materials, and cross sectional geometries, since the concrete plasticity model is intended to be used for many different applications. The papers are discussed individually in Section 6.1. The FE model predictions are compared to the test results in Section 6.2. A discussion of the overall performance of the FE model is in Section 6.3.

6.1 Test Data

Test data for confined concrete members are quite abundant; thus, it was possible to select test data similar to that which this FE model is intended to predict. A fairly broad spectrum was considered in the five papers. Both steel rebar and fiber reinforced polymer (FRP) confinement, as well as circular, square, and rectangular cross-sections, were included. Four of the papers presented results from axially loaded confined concrete members, while the fifth presented an axial load-moment strength interaction diagram. The set of papers is considered typical of what the FE model is designed to predict.

Chaallal and Shahawy (2000) studied the combined effects of axial and flexural loads on confined concrete members. The intent of the paper was to study the enhancement in strength by wrapping a lightly confined section in carbon fiber reinforced polymer (CFRP). The concrete was purchased from a commercial supplier with an experimentally determined compressive strength of 3.7 ksi (25.0 MPa) and a water-cement ratio of 0.68. The members tested were 8 x 14 x 84 inch (200 x 350 x 2100 mm) rectangular sections with 1 inch (25 mm) radius corners. Four Grade 60 number 6 bars ran longitudinally through the section. The hoops consisted of Grade 60 number 3 bars at 4 inches (100 mm). A cross section of the steel confined member, along with the material properties, is shown in Figure 6.1. The second member was identical to the first, but was wrapped with 2 plies of a bi-directional CFRP. Unfortunately, due to lack of information about the CFRP material and layout, the CFRP confined section could not be modeled. Hence, only the results for the hoop confined members are employed here. Pure axial load and pure moment were considered along with four intermediate axial load-moment combinations.

Harries and Carey (2003) observed the effect of cross sectional shape on performance. Two members with square cross sections, each with a different corner radius, and one member with a circular cross section were tested. The circular columns were 6 x 12 inch (152 x 305 mm) specimens, while the square columns were 6 x 6 x 12 inch (152 x 152 x 305 mm) specimens with either a 0.43 or 0.98 inch (11 or 25 mm) radius applied to the corners. The concrete had a compressive strength at testing of 4.6 ksi (31.8 MPa) for the cylindrical specimens, 4.1 ksi (28.6 MPa) for the square specimens with a 0.43 inch (11 mm) corner radius, and 4.7 ksi (32.4 MPa) for the square specimens with a 0.98 inch (25 mm) corner radius. All specimens were confined by three or six plies of E-glass FRP. The FRP had an experimentally-determined strength of 428 lb per inch per ply (75 N per mm per ply) and an elastic modulus of 28 kips per inch per ply (4.9 kN per mm per ply). The authors performed axial load tests on the specimens both with the FRP bonded to the member using epoxy as well as unbonded by covering the member with a kitchen-type plastic wrap before applying the FRP. Typical applications of composite confinement are bonded to the column,

so the unbonded tests were not used here.

Harries and Kharel (2003) investigated the effects of varying amounts and type of FRP confinement on axial behavior of confined columns. All specimens were 6 x 12 inch (152 x 305 mm) cylinders. The concrete had a compressive strength at testing of 4.7 ksi (32.1 MPa). Two different composite materials were used to create the FRP: a carbon fiber and an E-Glass fiber. The carbon fiber had an experimentally-determined strength of 994 lb per inch per ply (174 N per mm per ply) with an elastic modulus of 90 kips per inch per ply (15.7 kN per mm per ply). The E-Glass fiber had an experimentally-determined strength of 428 lb per inch per ply (75 N per mm per ply) and an elastic modulus of 28 kips per inch per ply (4.9 kN per mm per ply). The carbon FRP confined columns were tested with 1, 2, or 3 plies for confinement. The E-Glass FRP confined columns were tested with 1, 2, 3, 6, 9, 12, or 15 plies for confinement.

Mander et al. (1988a) tested the effect of steel rebar confinement on columns and walls. The columns were circular in cross section with dimensions of 19.7 x 59.1 inches (500 x 1500 mm), while the rectangular walls were 5.9 x 27.6 x 47.2 inches (150 x 700 x 1200 mm). All columns used in this comparison were loaded axially at a strain rate of 0.013 $\sec^{-1}$. This strain rate was utilized to simulate the rate of seismic loading. The unconfined compressive strength, determined at the 0.013 $\sec^{-1}$ strain rate, was 4.1 ksi (28 MPa). Mander et al. (1988b) states that loading at this strain rate will result in an increase in the stiffness, peak strength, and strain at peak stress. Thus, the unconfined compressive strength measured at this same strain rate of 0.013 $\sec^{-1}$ was designated as f'_c in the FE model. All walls used in this comparison were loaded axially at a strain rate of 0.00001 $\sec^{-1}$ and had a measured compressive strength, at that strain rate, of 3.8 ksi (26 MPa). All steel rebar used for longitudinal and confining steel was Grade 275. Scott et al. (1982) experimentally tested different rebar sizes, and the yield strength of the bars was found to vary with the size of the bar. These measured yield strengths were used in the FE model. Four columns were chosen for comparison. The columns all had twelve 0.63 inch (16 mm) diameter deformed longitudinal bars. Three were confined with spirals of 0.47 inch (12 mm)

diameter round bars at pitches of 1.61 to 4.06 inches (41 to 103 mm). The fourth was confined by a spiral of 0.39 inch (10 mm) diameter round bar at 4.69 inch (119 mm) pitch. Three different walls were used for comparison. All walls had sixteen 0.47 inch (12 mm) diameter deformed longitudinal bars. Transverse steel configurations were different for each of the three walls. All three consisted of hoops formed by 0.24 inch (6 mm) diameter round bars at either 0.98 or 1.97 inch (25 or 50 mm) spacing. The rebar configuration and material strengths for all columns and walls considered are shown in Figures 6.9 and 6.13.

Scott et al. (1982) studied square columns confined by steel rebar. All columns tested were 17.7 x 17.7 x 47.2 inches (450 x 450 x 1200 mm). Normal weight concrete was used. The concrete had a maximum aggregate size of 0.79 inches (20 mm) and a slump of 3 inches (75 mm). The cylinders were cured for 7 days at 68°F (20°C) and 100% humidity. They were then stripped and left standing in the laboratory for approximately five weeks before testing. Two confined columns were chosen for comparison which had a compressive strength, f'_c, for the concrete of 3.16 ksi (21.8 MPa). One column had twelve 0.79 inch (20 mm) diameter longitudinal bars with a yield strength, f_y, of 62.9 ksi (434 MPa). The other column had eight 0.94 inch (24 mm) diameter longitudinal bars with a yield strength, f_y, of 57.1 ksi (394 MPa). Both columns used 0.39 inch (10 mm) double hoops at a spacing of 2.84 inches (72 mm) having a yield strength of 44.8 ksi (309 MPa). The hoop configurations were different for the two columns. The cross sections and material properties are shown in Figure 6.16. Both columns were loaded axially at a strain rate of 0.0000033 sec^{-1}. Stress versus strain curves for various sizes of steel bars were determined in the paper and used for defining the yield strength of the rebar.

6.2 Comparison Results

6.2.1 Chaallal and Shahawy (2000)

The FE model was used to predict the axial load-moment interaction diagram of a hoop confined section, as tested in Chaallal and Shahawy (2000). The finite element mesh used to represent the section is shown in Appendix Section G.1. The comparison of the test results to the FE model prediction, along with the member cross section, is shown in Figure 6.1. At both the pure axial and balanced point loadings, the FE

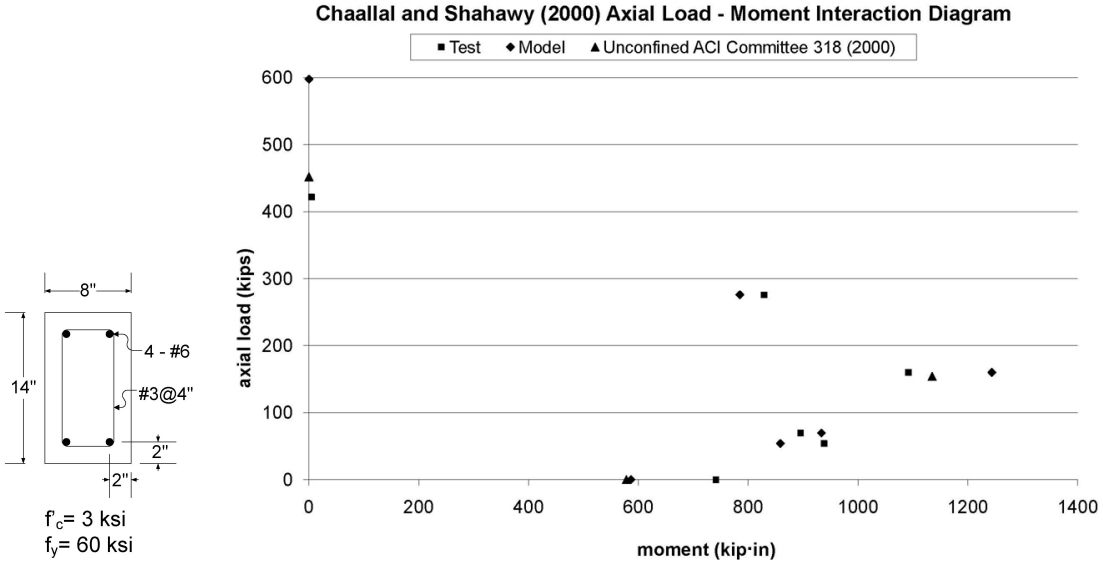

Figure 6.1: Comparison of model to test data from Chaallal and Shahawy (2000).

model appears to overestimate the experimental results. The balanced load point is defined as the point where the steel yields in tension at the same curvature that the concrete crushes under the compression. This balanced point will have the highest moment capacity of any axial load-moment combination. Assuming unconfined concrete and using equations from ACI Committee 318 (2000), the pure axial load supported by this column would be 452 kips (2012 kN), and the balanced moment would be 1135 kip·in (128.2 kN·m) at an axial load of 154 kips (685 kN). The experimental points lie below even this unconfined assumption. Thus, the experimental results at these points are not considered reliable. The opposite is observed at the pure moment point. For this case, the FE model is underestimating the experimen-

tal data. Again, assuming unconfined concrete and equations from ACI Committee 318 (2000), the pure moment that this section can withstand would be 578 kip·in (65.3 kN·m). The FE model prediction is 586 kip·in (66.2 kN·m). The FE model is predicting that the confinement is not effective under pure moment, which may be a reasonable assumption since the section will be partially cracked and the axial stress will vary over the uncracked portion. It is not clear what can be concluded from this comparison due to large discrepancies in the test results. The FE model may be overestimating the increase in strength for a lightly confined section. However, the test data clearly has some discrepancies, so the problems may not lie with the FE model.

6.2.2 Harries and Carey (2003)

Results from the testing of E-Glass FRP confined columns performed by Harries and Carey (2003) were compared to predictions from the FE model. The comparisons for the circular column and the two square columns are shown in Figures 6.2 through 6.4. The finite element meshes used to perform these predictions are shown in Appendix Section G.2. In Figure 6.4, the mismatch in the peak stress of the 0 ply column between the FE model and the test is due to the fact that the 0 ply column strength did not match the f'_c value specified in the paper.

The FE model predicts exceptionally well the behavior of the circular column. For the square columns, the experimental data suggest that there is sometimes slack in the loading mechanism. This type of variability in loading will not be accounted for in the FE model. However, the FE model does predict the peak stress of the specimen reasonably well. The square sections show a concave upward type behavior after the peak stress is reached. This behavior is not seen in the FE model, nor is it seen in the circular column. The physical mechanism leading to this abrupt drop is not discussed in the paper. Therefore, it is difficult to know whether there is a problem with the concrete plasticity model, a problem with the FE model, or a problem with the experimental results. There may be some features of the behavior

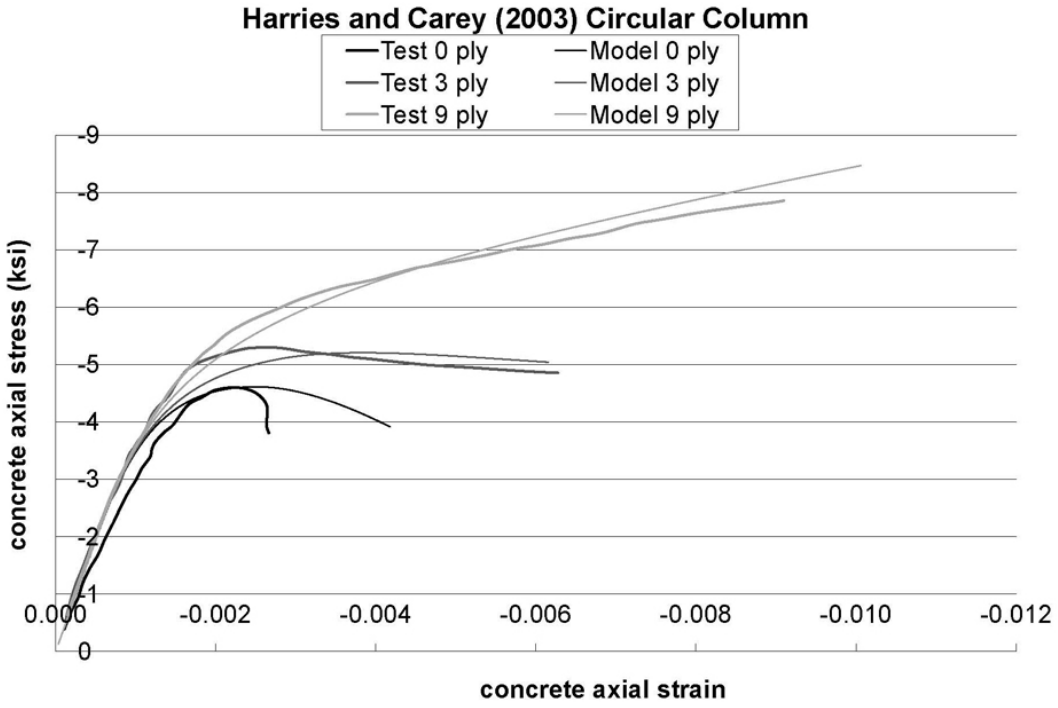

Figure 6.2: Comparison of model to test data from Harries and Carey (2003) for circular column.

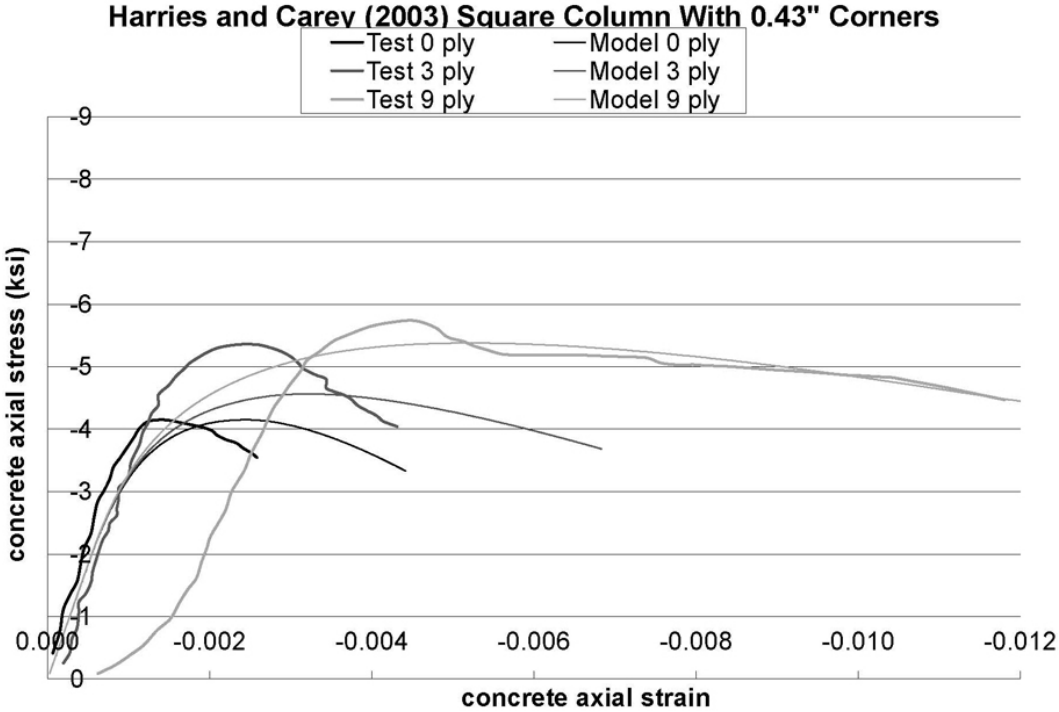

Figure 6.3: Comparison of model to test data from Harries and Carey (2003) for square column with 0.43 inch (11 mm) corner radius.

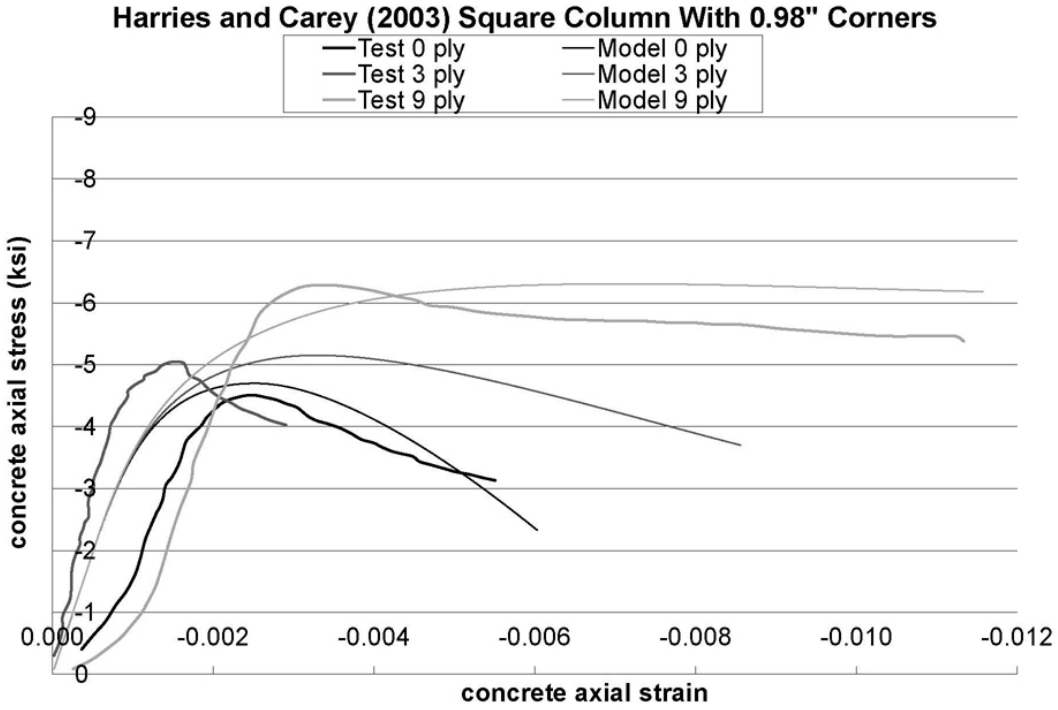

Figure 6.4: Comparison of model to test data from Harries and Carey (2003) for square column with 0.98 inch (25 mm) corner radius.

of square columns which are not captured by the FE model. However, since these shapes were again compared for steel confined sections, this issue will be discussed in conjunction with the results presented in Section 6.2.4.

6.2.3 Harries and Kharel (2003)

Experimental data for circular columns confined by two types of composites was given in Harries and Kharel (2003). In addition to the typical concrete axial stress versus strain data, the authors provided the dilation ratio of the column. The dilation ratio is defined as the ratio of the transverse strain to the axial strain. In order to compare transverse strains, the FE model was loaded to the point at which it reached the same axial strain as the experiment. In some cases, the FE model predicted composite rupture before it reached the final experimental axial strain. These cases are denoted by an asterisk (*) in the figures. Comparison of the carbon FRP confined columns is shown in Figures 6.5 and 6.6. Results of the E-glass FRP confined columns are

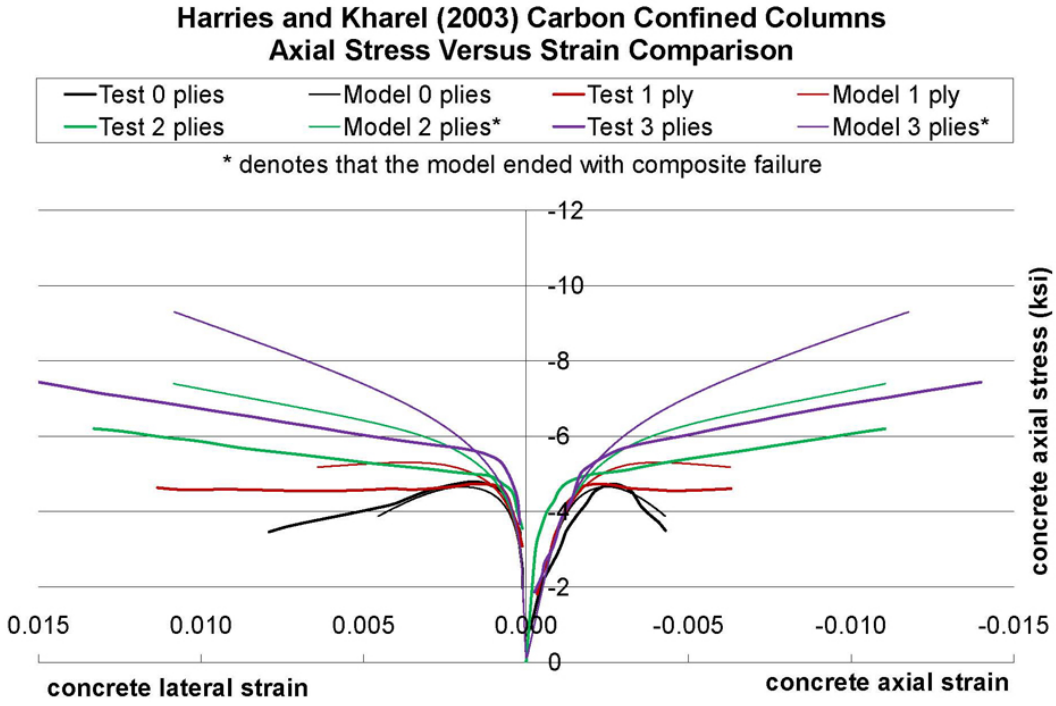

Figure 6.5: Axial stress versus strain comparison of model to test data from Harries and Kharel (2003) for columns confined by carbon FRP.

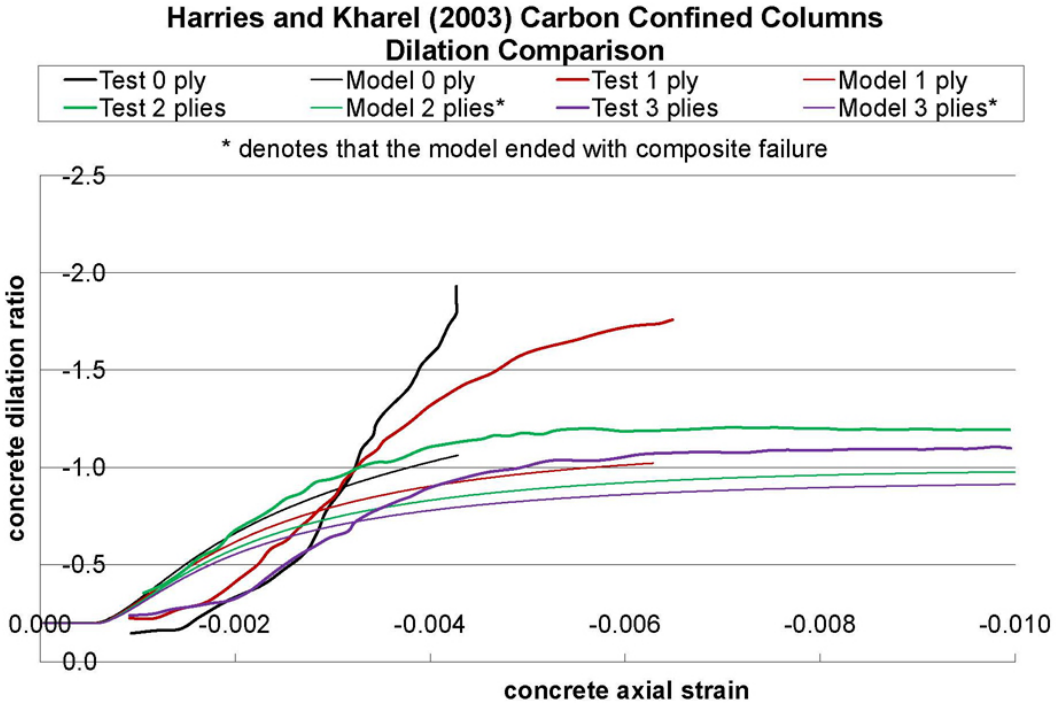

Figure 6.6: Dilation ratio comparison of model to test data from Harries and Kharel (2003) for columns confined by carbon FRP.

compared in Figures 6.7 and 6.8. The mesh used to generate the FE results is shown

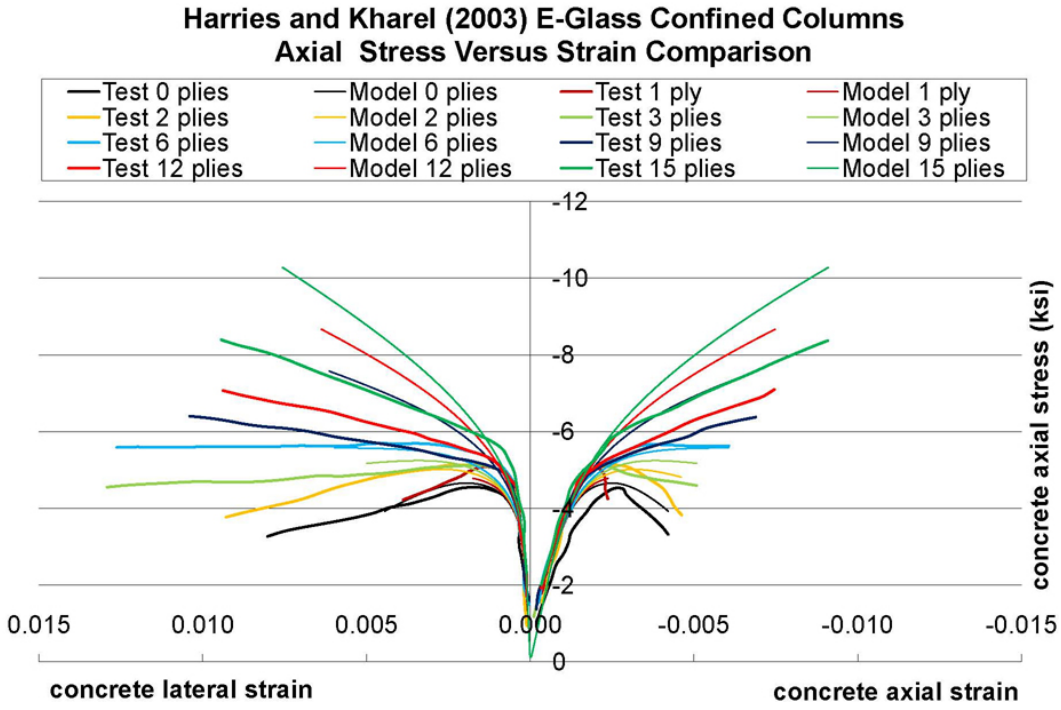

Figure 6.7: Axial stress versus strain comparison of model to test data from Harries and Kharel (2003) for columns confined by E-glass FRP.

in Appendix Section G.3.

For the carbon FRP confined columns, the FE model appears to consistently overestimate the increase in strength with confinement. However, it also underestimates the amount of transverse strain that the column should exhibit. It would be expected that if the FE model were underestimating the transverse strains of the specimen, it would also underestimate the strains in the confining material and, thus, underestimate the strength increase. The fact that the FE model underestimates the transverse strain but overestimates the strength implies that the stiffness of the confining material provided by the paper is too large. This idea is reinforced by the fact that for lower levels of E-glass confinement (where the confining material behavior will not affect the results as significantly), the strength increase in the FE model is somewhat closer to that predicted by the experiment. However, it must also be noted that the overestimate of the strength and underestimate of the transverse strains are consistent between the two different confining materials found in the paper. Thus, while it

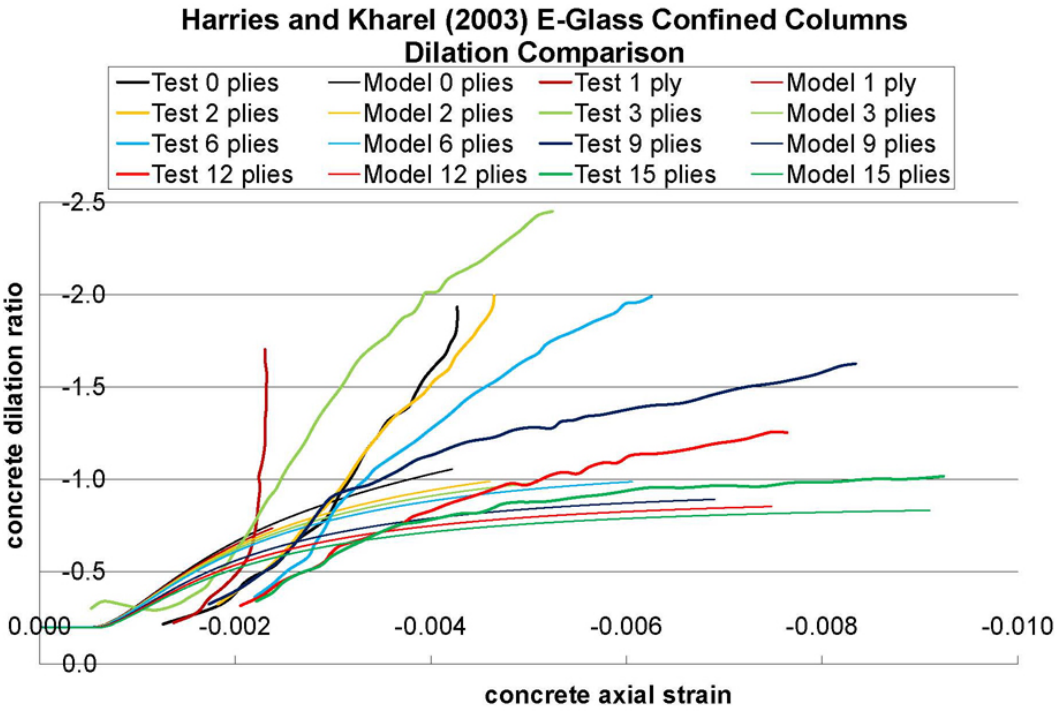

Figure 6.8: Dilation ratio comparison of model to test data from Harries and Kharel (2003) for columns confined by E-glass FRP.

may still be the case that the manufacturer overestimated the composite properties for both types of fiber, it may also be the case that the FE model is not predicting the behavior of this concrete mix very well. Examining the FE model prediction for the unconfined columns shows that it is also underestimating the transverse strains for that unconfined case.

This paper and Harries and Carey (2003) used the same E-glass FRP for confinement. The FE model performed exceptionally well at predicting the behavior of the circular columns confined by the E-glass FRP in Harries and Carey (2003). Thus, it would seem that the composite properties are well defined for that case. It may be the case, physically, that the ply effectiveness is decreased with an increasing number of plies due to the increase in the final thickness of the FRP. This would mean that the strength increase from one ply to two plies would be more significant than the strength increase from, for example, 12 plies to 13 plies. Unfortunately, the data at lower confinement levels exhibit some discrepancies. In the case of the Carbon FRP, no strength increase is exhibited by the addition of the first ply. In the case of the

E-Glass FRP, the 1, 2, and 3 ply results exhibit the same peak stress, which is higher than the unconfined peak stress. Due to these inconsistencies in the test data at lower confinement levels, it is difficult to see the increase in strength with each ply. However, if it is a valid assumption that the ply effectiveness is decreased with an increasing number of plies, this effect is not accounted for in the FE model and could lead to the fact that the strength overestimation is more severe at higher ply counts.

The FE model does reasonably well predicting the data, particularly considering that the data is not consistent for low ply counts. Thus, it is considered that the errors seen between the FE model and the experiments are not significantly larger than the errors that can be seen in the experiments themselves.

6.2.4 Mander et al. (1988a)

Both circular columns and rectangular walls were tested by Mander et al. (1988a). The FE model was used to predict four different columns and three different walls. The FE meshes used are shown in Appendix Section G.4. The cross section and rebar configuration for the four circular columns is shown in Figure 6.9. It should be

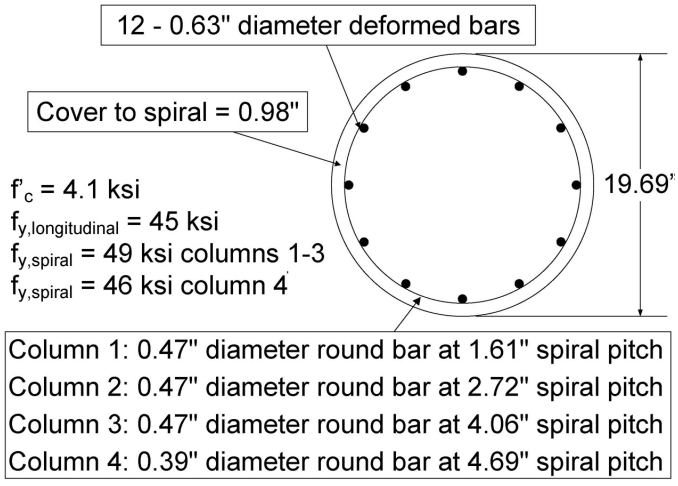

Figure 6.9: Details of circular columns tested in Mander et al. (1988a) and predicted using the current model.

noted that a difference between the FRP tests and the steel rebar confined tests is the presence of cover concrete. It is expected that the concrete external to the steel

hoops or spirals will spall off and become ineffective at strains higher than the axial concrete strain at peak uniaxial stress. The model should properly account for this effect. A comparison of the FE model prediction to the experimental data is shown in Figure 6.10. The FE model predictions do not extend to the same axial strain as

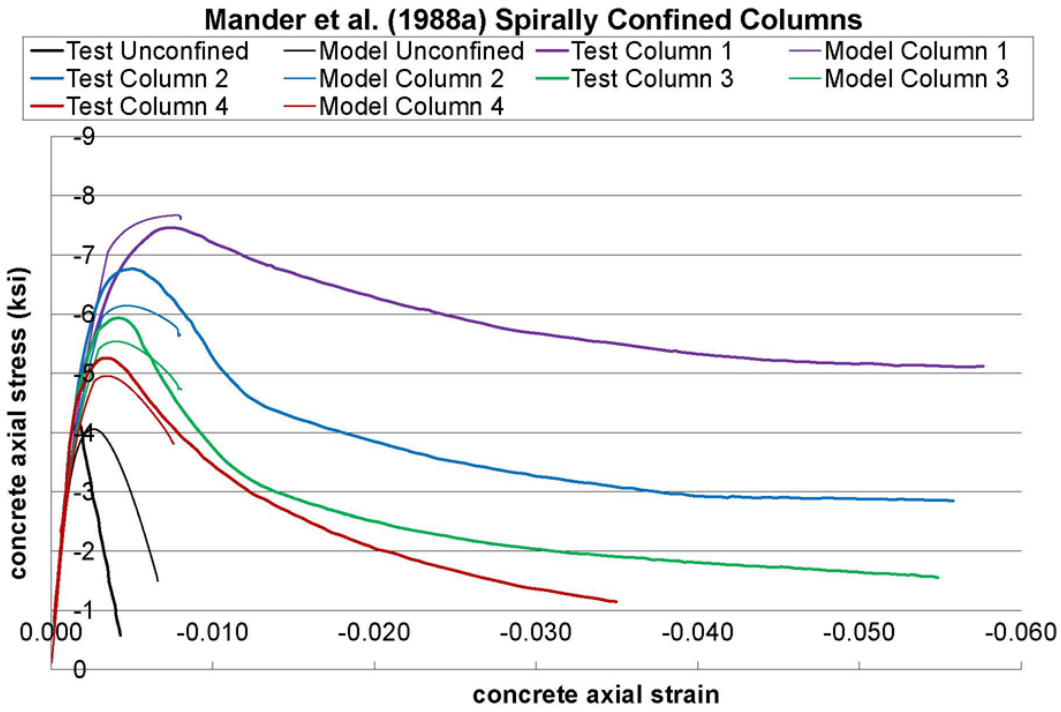

Figure 6.10: Comparison of model to test data from Mander et al. (1988a) for circular columns.

the test data. While the FE model successfully predicted strain softening in the case of the FRP confined sections, it stops converging not long after the peak stress in the steel rebar confined case. However, it was discovered that if the tensile meridian of the residual surface was set to be equal to that of the compression meridian, the FE model would continue on to the desired strain levels. It is not apparent why this change fixes the convergence problem. Fundamentally, a nonlinear problem with strain softening is extremely sensitive and finding a reliable iteration method can be extremely difficult. Further, recall from Section 4.3, no data was found for the tensile meridian of the residual surface. An assumption was made that the ratio of the parameters for the compressive and tensile meridians between the peak and residual surface would be the same. There is no physical basis for that particular assumption.

Therefore, there is also no data to refute the assumption that the residual surface is round. Thus, the concrete model, altered to have a round residual surface, was implemented into the FE model and used to predict the column data. Results for this case are shown in Figure 6.11. The spiral strains were given for column 4 and

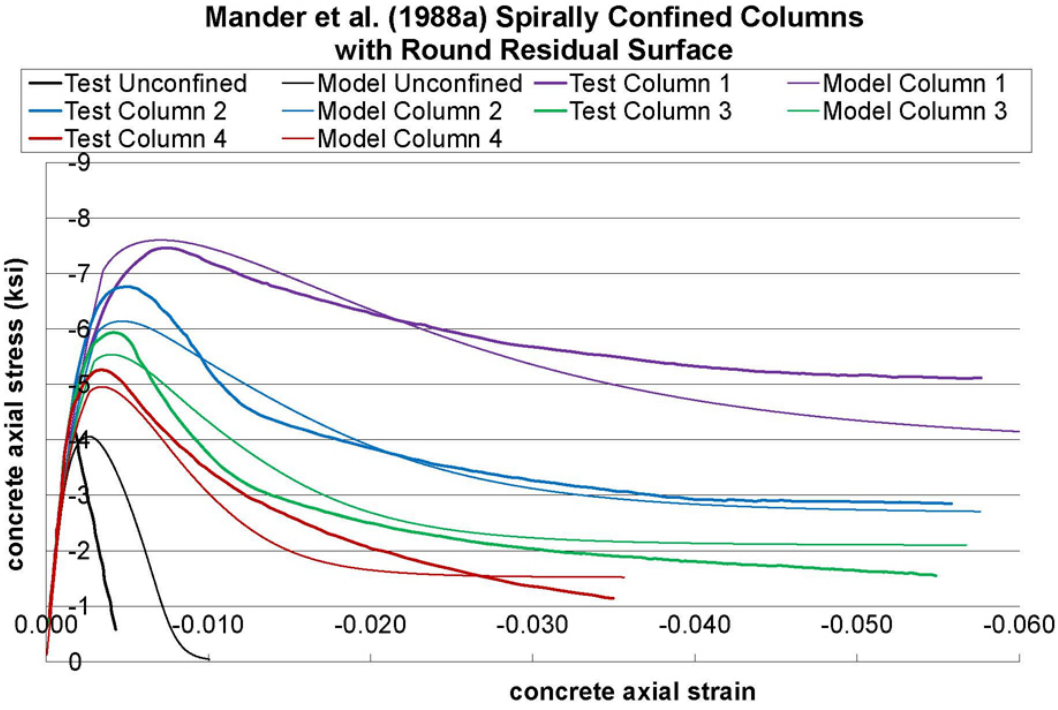

Figure 6.11: Comparison of model with round residual surface to test data from Mander et al. (1988a) for circular columns.

are compared to FE model predictions in Figure 6.12. Up to the peak stress of the concrete, the results will be identical for the two different residual surfaces. Use of a round residual surface is expected to overestimate the residual strength of the concrete for cases where the Lode angle is less than 60°. However, for circular columns, the theoretical Lode angle will be close to 60° throughout the specimen because the two lateral in-plane stresses are roughly equal. Thus, it is not expected that the concrete model with a round residual surface will differ much in prediction from the concrete model originally defined in Chapter 3.

The FE model does quite well at predicting the strain at peak stress. However, it underestimates the peak stress increase due to confinement for the circular columns except for the case with highest confinement. This may be due to the strain rate

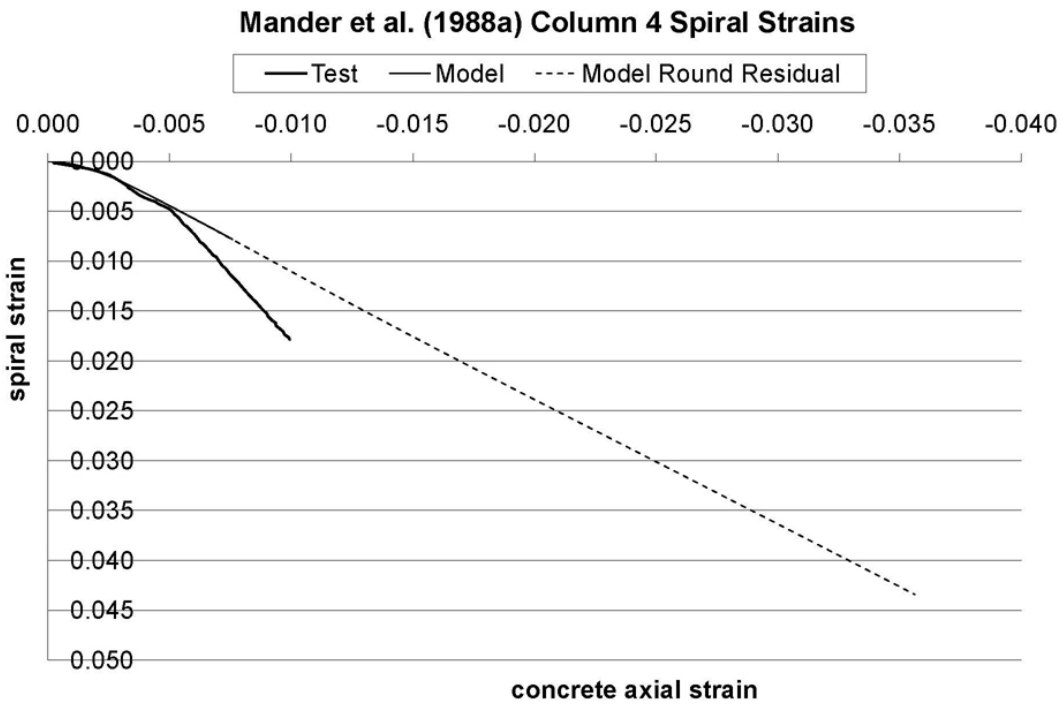

Figure 6.12: Comparison of FE model to test data from Mander et al. (1988a) for column 4.

of 0.013 $\sec^{-1}$ at which the columns were tested. As mentioned in Section 6.1, the concrete stiffness, peak strength, and strain at peak stress are increased when loading at a strain rate of 0.013 $\sec^{-1}$. This higher value for f'_c was used for the FE model. However, it appears that how the peak strength increases with confinement may also be affected by rapid loading, which is not accounted for in the FE model. Scott et al. (1982) measured a larger strength increase due to confinement at a strain rate of 0.0167 $\sec^{-1}$ than the strength increase at a strain rate of 0.0000033 $\sec^{-1}$. Thus, it is this dynamic loading effect which is most likely leading to the discrepancy in peak stress, as the concrete model presented in this thesis does not account for strain rate effects.

The FE model does exceptionally well at predicting the spiral strains up to the peak stress of the concrete. In the strain softening portion, the FE model appears to be underestimating the spiral strains. The concrete axial strain at peak stress is approximately 0.0034. Thus, it would appear that the FE model is underestimating the post-peak volumetric expansion for this column.

The cross section and rebar configuration for the three different walls are shown in Figure 6.13. The experimental results are compared to the FE model predictions

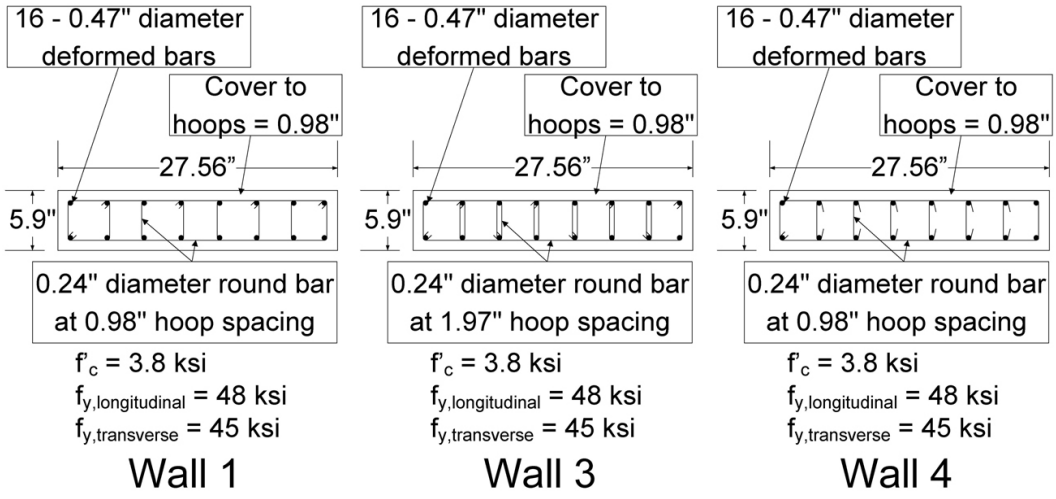

Figure 6.13: Details of rectangular walls tested in Mander et al. (1988a) and predicted using the current model.

for the walls in Figure 6.14. Note that wall 8 was one of four unconfined walls tested by Mander et al. (1988a). This wall had no longitudinal or transverse steel. As with the circular columns, the identical problem was encountered with the walls: the FE model was not able to predict the post-peak behavior of the rectangular walls. The concrete model was again modified to have a round residual surface, and the FE model was then able to successfully predict the strain softening behavior of the walls. However, for the rectangular walls, it is expected that the Lode angle will be different than 60°, as was the case for the circular columns. Therefore, it is expected that the residual strength of the walls will be slightly overestimated by using a round residual surface compared to the residual surface laid out in Chapter 3. However, recall that there is no data for a Lode angle of 0°, so it is not known which residual surface more closely represents concrete.

The FE model prediction with the round residual surface is compared to experimental results in Figure 6.15. The FE model is not as successful at predicting the behavior of the walls as it was with the circular columns. However, a review of the experimental data may reveal the cause of some of the discrepancies. Wall 3 had

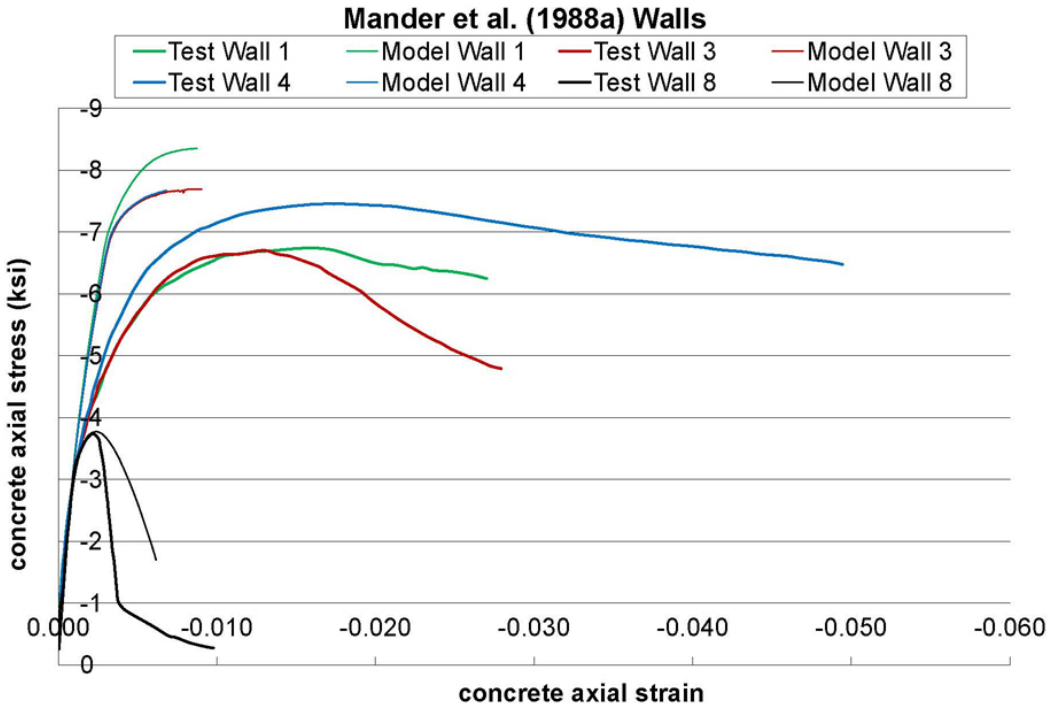

Figure 6.14: Comparison of model to test data from Mander et al. (1988a) for rectangular walls.

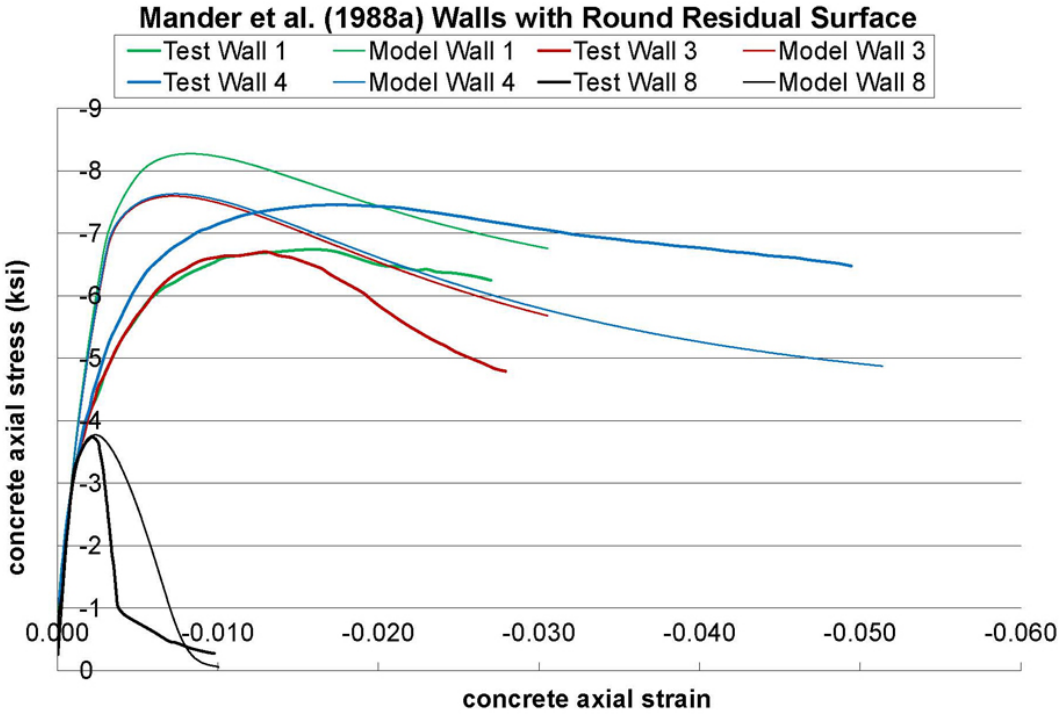

Figure 6.15: Comparison of model with round residual surface to test data from Mander et al. (1988a) for rectangular walls.

twice as much transverse steel as wall 4, but with twice the hoop spacing. Thus, it is expected that their behaviors may be similar. Wall 1 had more transverse steel than wall 4, but with the identical hoop spacing. Therefore, it is expected that wall 1 will support a higher concrete stress then wall 4. However, these results are not seen in the experimental testing. Mander et al. (1988a) noted that an unexpected issue with wall buckling likely led to the premature failure of wall 1. Thus, similar testing issues may have lead to the discrepancies seen in predicting the peak stress. It is clear that the FE model is also underestimating the strain at peak stress for all of these walls. The FE model also appears to soften more rapidly than the experiments. This is likely due to the absence of strain hardening in the steel model. The effects of not modeling strain hardening in the rebar will be illustrated further in Section 6.2.5.

6.2.5 Scott et al. (1982)

Two square columns tested by Scott et al. (1982) were compared to predictions made by the FE model, using the FE meshes shown in Appendix Section G.5. The cross section and rebar details for these two columns are shown in Figure 6.16. A compar-

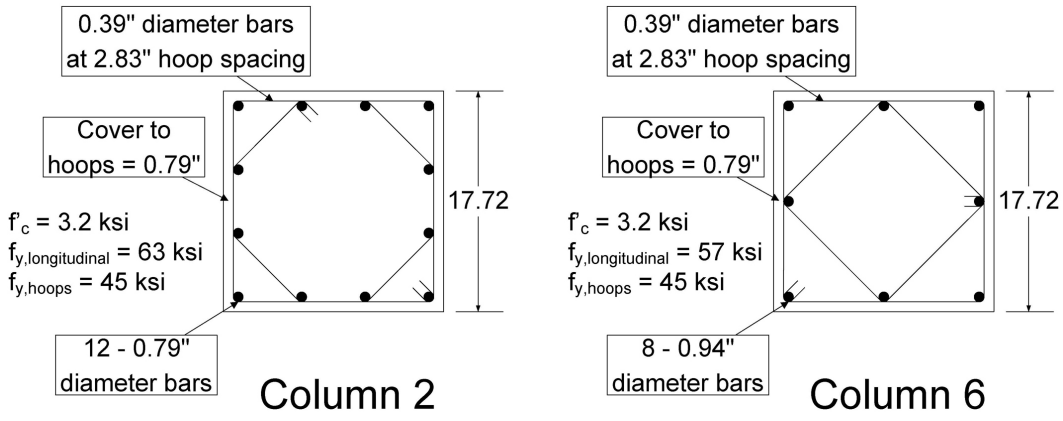

Figure 6.16: Details of square columns tested in Scott et al. (1982) and predicted using the current model.

ison of the experimental results to the FE model predictions is shown in Figure 6.17. Note that column 1 was an unconfined specimen and, therefore, had no longitudinal or transverse steel. The same problem discussed in Section 6.2.4 was encountered

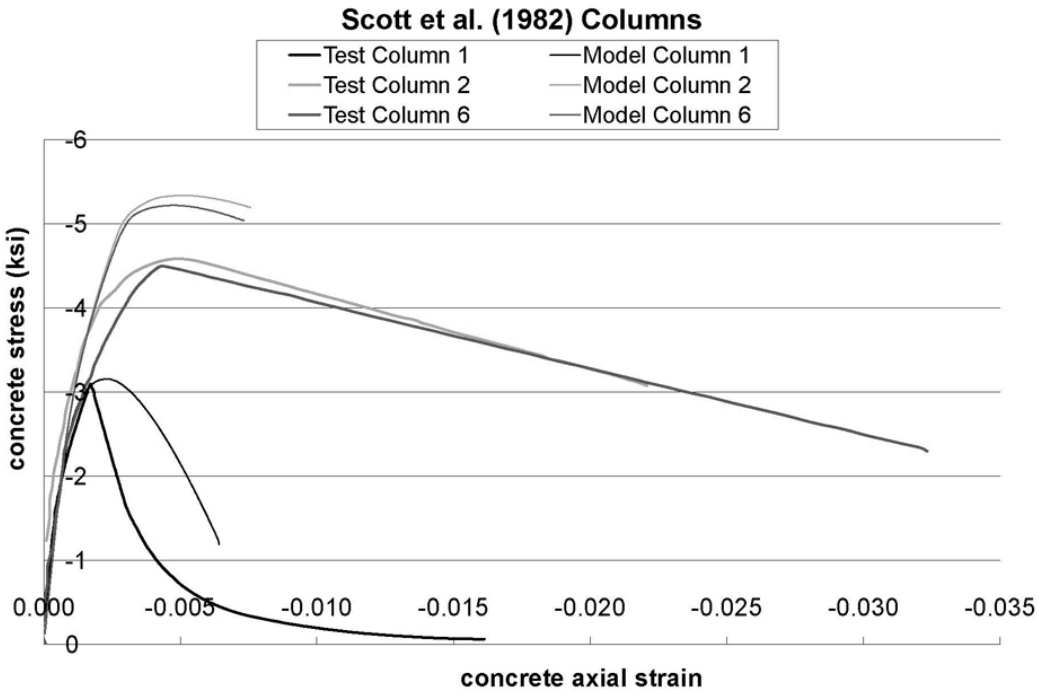

Figure 6.17: Comparison of model to test data from Scott et al. (1982) for square columns.

with this data: the FE model is not able to predict the strain softening region. The concrete model was again altered to have a round residual surface, and the results are compared in Figure 6.18. While the strength is overestimated for both columns, the FE model does an excellent job at predicting the difference in strength due to the different transverse rebar configurations. While the performance difference is small, the ability of the FE model to accurately capture it shows that the FE model is able to predict the way in which confinement affects the strength and ductility of the concrete, which was its core purpose.

Scott et al. (1982) also provided plots of the concrete and longitudinal steel forces as well as the average hoop stresses for each of these two columns. These are compared to the FE model predictions in Figures 6.19 through 6.22. Here, it is apparent how well the FE model is able to predict the concrete expansion which engages and loads the steel rebar. The strain softening appears to occur too quickly in the FE model, but this is likely due to the absence of strain hardening in the steel model. The strains at which steel strain hardening begins to take place in the experiment is where the

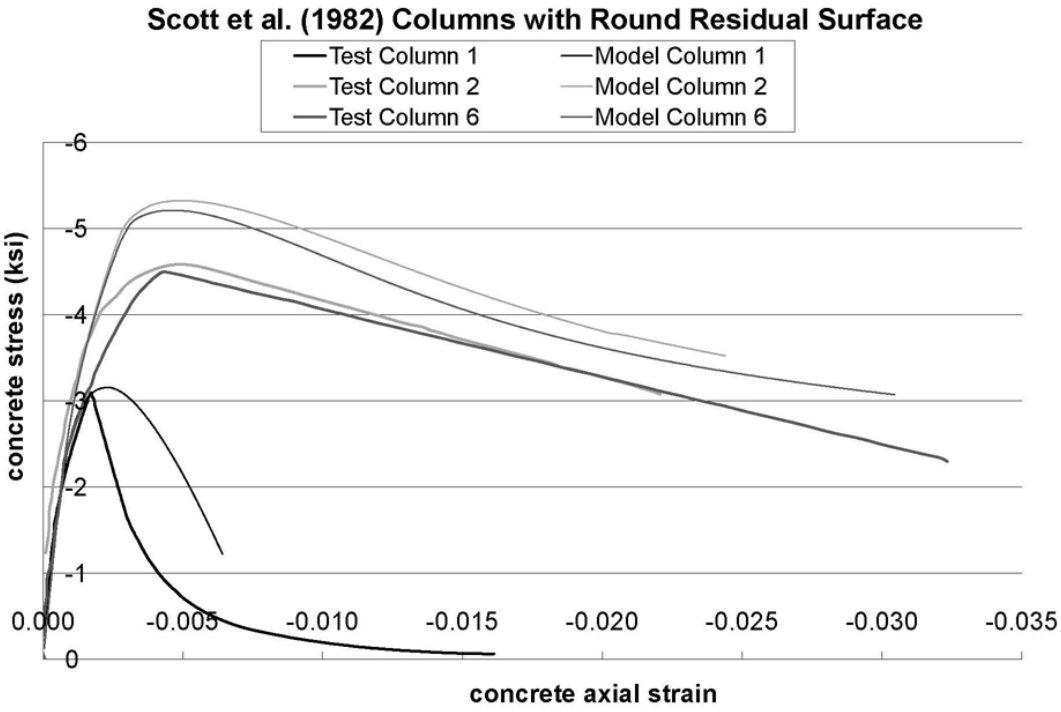

Figure 6.18: Comparison of model with round residual surface to test data from Scott et al. (1982) for square columns.

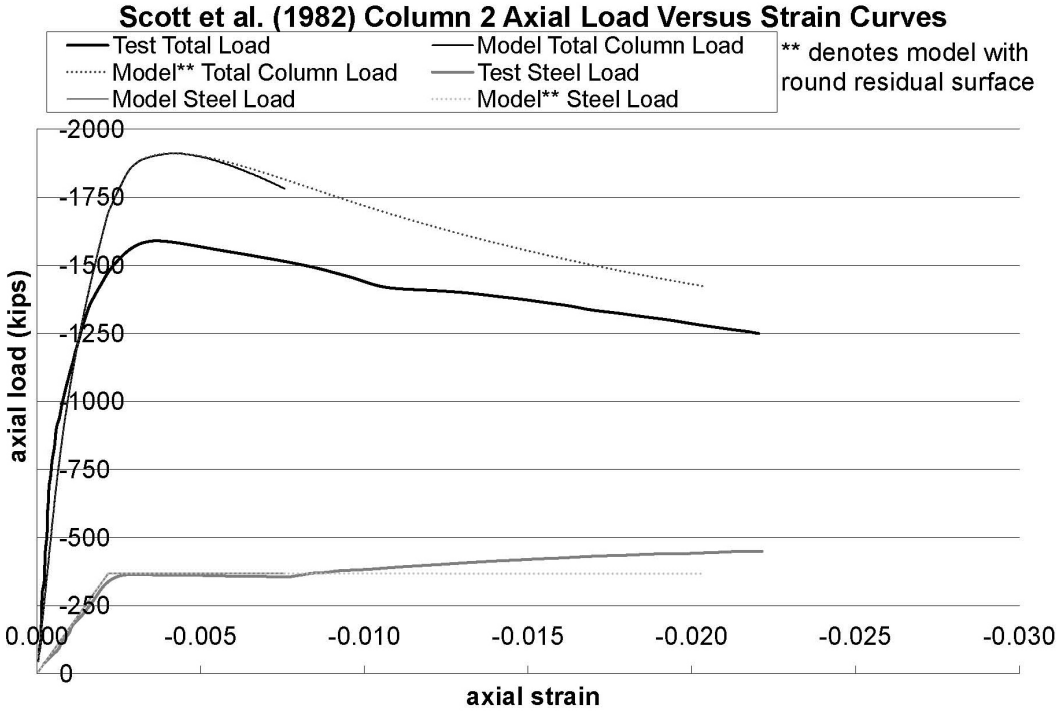

Figure 6.19: Comparison of model to test data from Scott et al. (1982) for column 2 concrete and steel forces.

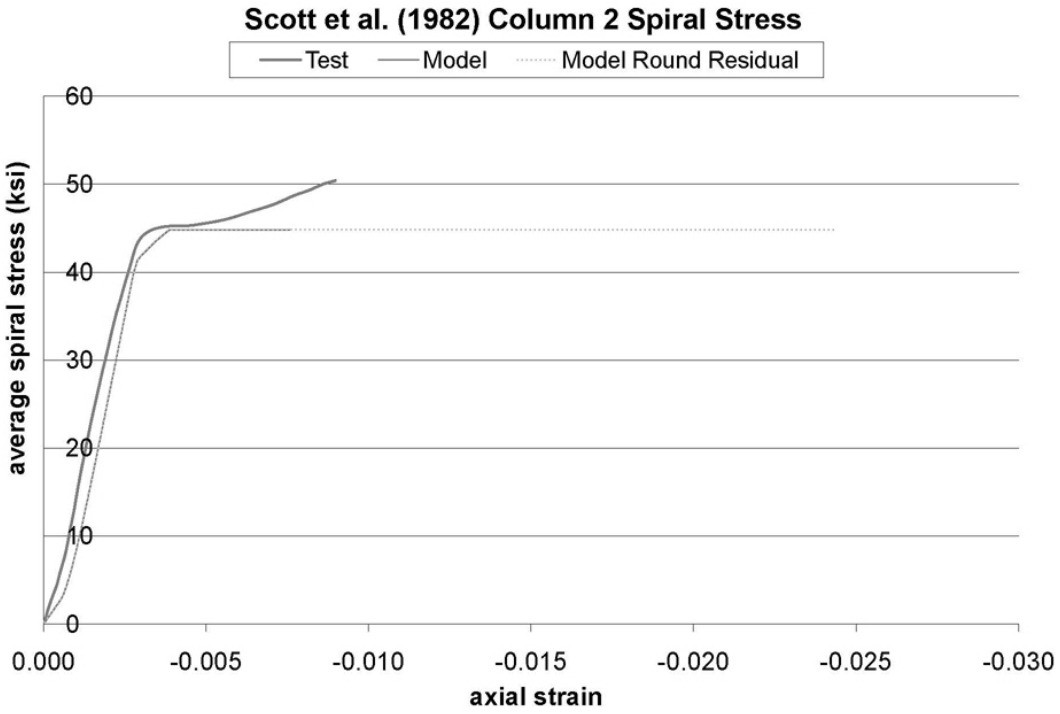

Figure 6.20: Comparison of model to test data from Scott et al. (1982) for column 2 hoop stresses.

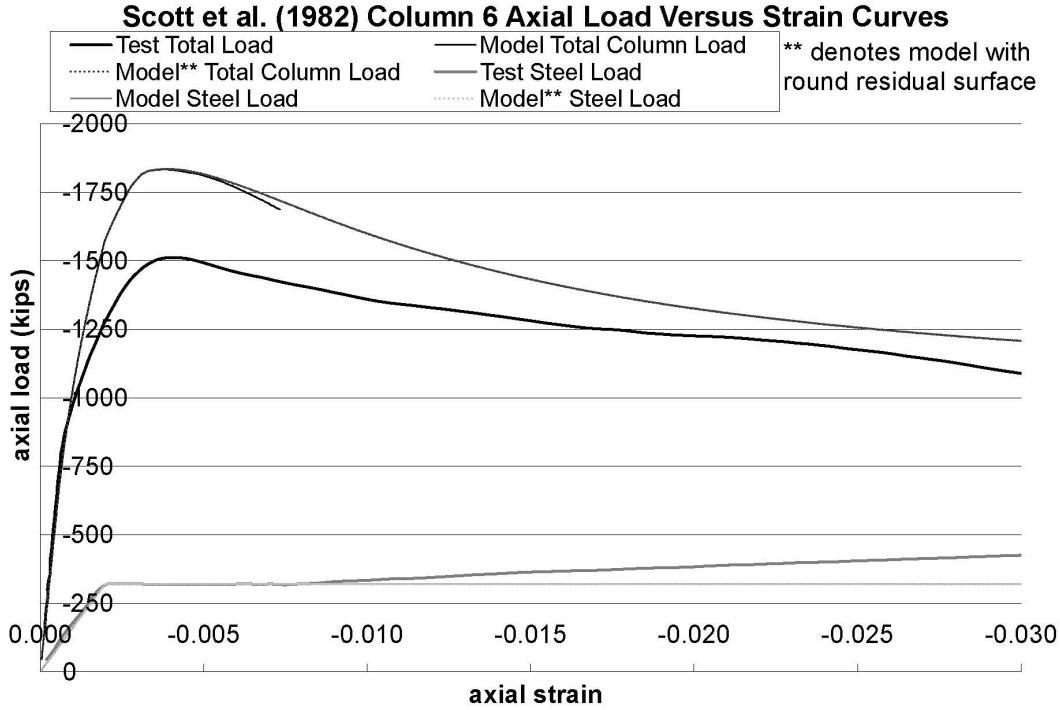

Figure 6.21: Comparison of model to test data from Scott et al. (1982) for column 6 concrete and steel forces.

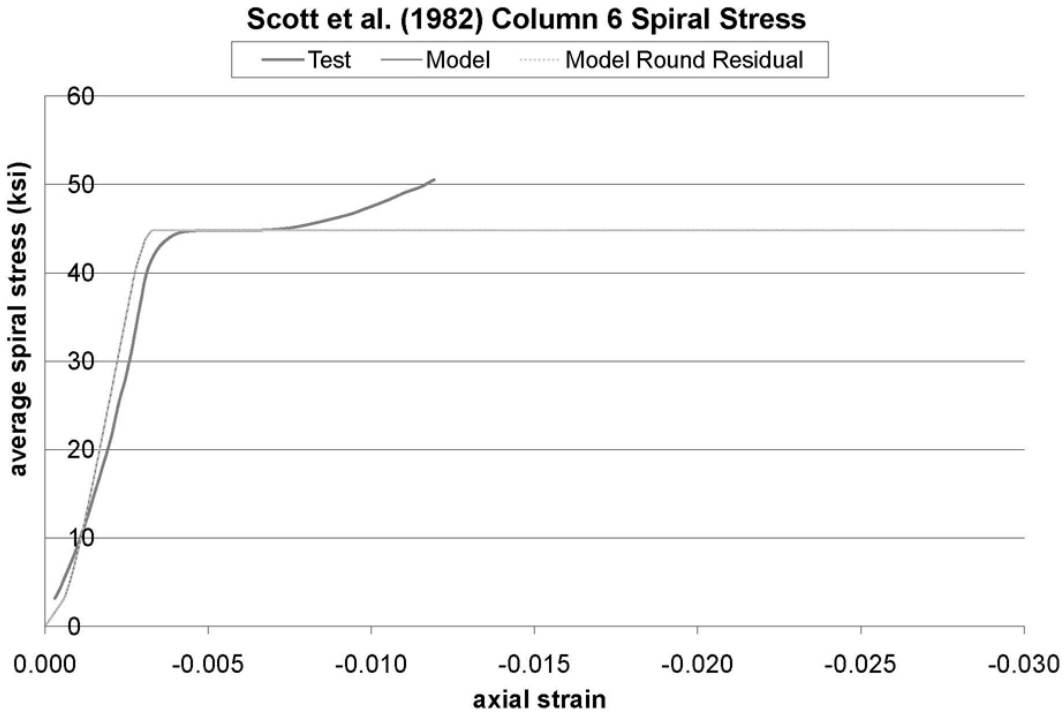

Figure 6.22: Comparison of model to test data from Scott et al. (1982) for column 6 hoop stresses.

FE model continues to soften more rapidly than seen in the experiments. If strain hardening were to be introduced into the steel model, the FE model predictions may fall at nearly the same rate as the experiments show. Thus, although the FE model over-predicts the strength for this case, all other behaviors are predicted extremely well by the concrete model.

6.3 Conclusions from the Comparisons

It is well established that variability in the behavior of concrete can be quite substantial (Nilson, 1997). Due to the variability within each material used to create the mix, the process by which it is created, the change in the concrete with age and loading, and the fact that concrete is a congeries of different materials, the strength, stiffness, and other overall properties of concrete will vary. For these reasons, it is difficult to consistently predict the behavior of concrete when the material itself does not behave consistently. For most modeling comparisons, the ideal is to have the prediction lie

within a few percent of the tests; this is not possible for concrete. Several experiments performed identically on the same batch of concrete specimens typically will not lie within a few percent of each other [for example, Bresler and Pister (1958), Duke and Davis (1944), and Hurlbut (1985)]. This must be appreciated when comparing a computer model to the somewhat erratic experimental data for concrete.

The FE model is able to predict concrete behavior under a wide range of loading and confinement types. There is no consistent error observed in any predicted quantity; an overestimate in a particular quantity on one set of data will be an underestimate on a different set. With the FRP confined circular columns, the FE model shows an overestimation of the observed strength, whereas for the circular steel confined columns, the FE model underestimates the observed strength. The FE model prediction of the square FRP confined columns tends to overestimate the experimental strain at peak strength, while the prediction for the steel confined walls underestimates this quantity. The remaining experiments showed close agreement in the experimental strain at peak stress. Thus, the FE model does not appear to be flawed in some fundamental way that would lead to a consistent difference between experiments and model predictions.

More significantly, the FE model is able to capture the changes in concrete behavior brought about by changes in shape, confining material, steel confinement configuration, and other experimental variables. While the FE model prediction of the square FRP confined columns of Section 6.2.2 shows a difference in the shape of the axial stress versus strain curves, the FE model predicts the curves for the square rebar confined columns of Section 6.2.5 reasonably well. Also, the FE model is able to predict the behavior of circular columns quite well. Thus, it is shown that the FE model can successfully predict concrete behavior for both square and circular cross sections. Further, the FE model is able to represent the concrete behavior with both FRP confinement and steel rebar confinement. The circular cross sections in Section 6.2.3 show a transition from post-peak strain softening to strain hardening. This transition is predicted by the FE model. The small increase in peak stress with a change in transverse steel configuration in Section 6.2.5 is also seen in the FE model

predictions. Thus, the FE model is able to predict concrete behavior confined by two quite different confinement materials.

The experimental data in Section 6.2.1 proved to have some obvious discrepancies. The unconfined ACI equations were able to predict the behavior better than the FE model. While the section was lightly confined, some effect of confinement would be expected. However, none was seen in the experimental results. Thus, issues with the data made it impossible to draw any conclusions about the accuracy of the FE model predictions. More data of this type is needed for comparison before the FE model can be considered accurate in predicting axial load-moment strength interaction diagrams.

The FE model was designed to account for a variety of different loading configurations (confinement material, geometry, loading type, etc.) so that the behavior of concrete under these conditions could be studied. While it is unfortunate that the original concrete model has an unknown issue that prevents prediction of the full strain softening region for steel confinement, use of the round residual surface appears to be a satisfactory substitute until the issue can be resolved. Overall, the FE model is considered to perform adequately for predicting the axial load behavior of confined sections.